Published by :
http://www.ijert.org

International Journal of Engineering Research & Technology (IJERT)
ISSN: 2278-0181
Vol. 5 Issue 01, January-2016

Comparative Analysis of Turbo Parameters at Variable Speed in Off Line Mode

M. Olubiwe
Dept of Electrical and Electronic Engineering,
Federal University of Technology
Owerri, Nigeria

Abstract **- The design of a robust coupling for study, for dynamic performance of a synchronous generator requires an accurate dynamic model of the driving and the driven part of the entire design. In this paper, a new procedure for identifying the parameters under varying speed condition of a synchronous generator has been developed. It will be shown that the parameters of this model can be easily identified from offline mode of the generator. The validity of the theoretical model has been verified by comparing results from simulated oscillograms with analytical method from well known equations. The design was simulated with rubber, steel and rigid coupling respectively. The result of the variable speed simulation and that of constant speed were also compared. The results showed that with constant speed simulation at the time of sudden short circuit (ssc) the subtransient and the transient decayed rapidly to steady state condition, while under the influence of variable speed, it took longer time before the subtransient and transient short circuit current to come to steady state, thereby causing heavy oscilation in the machine. This paper has shown that with good coupling design, parameters of a turbo generator can be captured at a variable speed condition and compared**

Key Words: Coupling, Dynamic, Parameters, Synchronous generator, Variable-speed

I INTRODUCTION

Knowledge of the operational parameters of synchronous machines is vital for reliable stability studies and "post mortem" analyses. Having accurate models of dynamic elements (including synchronous machines and other power plant controllers) is very important for optimal decision making, planning, and efficient operation of the power grid. Parameters of generators may differ from those in the utility's database due to aging processes, magnetic saturation, or changes of temperature during machine operation [1], [2]. As a matter of fact, many utilities around the world still use machine model parameters calculated during generator commissioning, leading to substantial differences between the actual and simulated dynamic behavior. AS power systems become more interconnected and complicated, analysis of dynamic performance of such systems becomes more important. Synchronous generators play a very important role in the stability of power systems. A valid model for synchronous generators is essential for a valid analysis of stability and dynamic performance. Almost three quarters of a century, after the first publications in modelling synchronous generators **[3], [4]**, the subject is still a challenging and attractive research topic.

The first and traditional methods of modelling of synchronous generators are well specified in IEEE standards **[5]**. These methods assume a known structure for the synchronous machine, using well-established theories like Park transformation. The drive system consist of two DC motors each with per unit rotor inertia J_{DC} and the driven synchronous generator with rotary inertia J_{GEN}. Both motors drive a gear train with ratio K, which in turn drives the generator. The generator is coupled to the gear train with an elastic coupling of torsion spring coefficient C in between them.

Before the analysis of variable speed, it is important to recall the basic d-q-0 equations to aid in the simulations.

$$\frac{di_a(\tau)}{d\tau} = \frac{1}{l_a}\left[V_a - r_a i_a(\tau) - K\psi\omega_m(\tau)\right] \qquad (1)$$

$$\frac{d\omega_m(\tau)}{d\tau} = \frac{K\psi i_a(\tau) - T_{SH}(\tau)}{J_{EFF-DC}} \qquad (2)$$

Where

i_a (τ) and ω_m (τ)are respectively, the armature current and rotor speed.

τ is per unit time.

r_a and l_a are the machine reactance and inductance in p.u.

ψ is the armature flux.

K is the constant determined by the design of the armature winding.

International Journal of Engineering Research & Technology (IJERT)
ISSN: 2278-0181
Vol. 5 Issue 01, January-2016

$J_{EFF\text{-}DC}$ is the per unit moment of inertia of the entire moving mass comprising the DC motor rotor and the rotor of the synchronous generator as seen from the motor side.

$$V_{ds} = r_s I_{ds} + \frac{d\lambda_{ds}}{d\tau} - \omega_r \lambda_{qs} \qquad (3)$$

$$V_{qs} = r_s I_{qs} + \frac{d}{d\tau}\lambda_{qs} + \omega_r \lambda_{ds} \qquad (4)$$

$$V_{fr} = r_{fr} I_{fr} + \frac{d}{d\tau}\lambda_{fr} \qquad (5)$$

$$0 = r_{dr} I_{dr} + \frac{d}{d\tau}\lambda_{dr} \qquad (6)$$

$$0 = r_{qr} I_{qr} + \frac{d}{d\tau}\lambda_{qr} \qquad (7)$$

Where the flux linkages are

$$\begin{bmatrix} \lambda_{qs} \\ \lambda_{ds} \\ \lambda_{qr} \\ \lambda_{dr} \\ \lambda_{fr} \end{bmatrix} = \frac{1}{\omega_r} \begin{bmatrix} X_{qr} & 0 & X_{mq} & 0 & 0 \\ 0 & X_{ds} & 0 & X_{md} & X_{md} \\ X_{mq} & 0 & Xqr & 0 & 0 \\ 0 & X_{md} & 0 & X_{dr} & X_{md} \\ 0 & X_{md} & 0 & X_{md} & X_{fr} \end{bmatrix} \times \begin{bmatrix} 1_{qs} \\ 1_{ds} \\ 1_{qr} \\ 1_{dr} \\ 1_{fr} \end{bmatrix} \qquad (8)$$

Where

$X_{qs} = X_{mq} + X_{ls}$

$X_{ds} = X_{md} + X_{ls}$

$X_{qr} = X_{mq} + X_{lqr}$

$X_{dr} = X_{mq} + X_{ldr}$

$X_{fr} = X_{md} + X_{lfr}$

The speed and torque are related by

$$\frac{d}{d\tau}\omega r = \left(\frac{T_{EX} - T_L}{J_{GEN}}\right) \qquad (9)$$

The torque is given by

$$T_{EX} = \frac{3}{2}\frac{P}{2}\left(\lambda_{ds} I_{qs} - \lambda_{qs} I_{ds}\right) \qquad (10)$$

All parameters have their meanings in p.u. of the rated base conditions.These equations are complete, there is need to deduce the state variables which can easily be obtained by noting that at no-load condition, the rotor is operating at rated synchronous speed, the rotor and stator currents I_{dr}, I_{qr}, I_{qs} and I_{ds} are nominally zero.

Hence, the flux linkages in equation (8) becomes:

$$\lambda_{ds} = \lambda_{dr} = \frac{X_{md} I_{fr}}{\omega_r} \qquad (11)$$

$$\lambda_{fr} = \frac{X_{fr} I_{fr}}{\omega_r}$$

$$\lambda qs = \lambda qr = 0$$

With equation (11), equation (3) now become

$$V_{ds} = \frac{d}{d\tau}\lambda_{ds} = \frac{X_{md}}{\omega_r}\frac{d}{d\tau} I_{fr} = 0 \text{ (since } I_{fr} \text{ is a dc current)} \qquad (12)$$

However, under steady-state no-load condition the terminal voltage Vs is 1.0p.u. and is given by

$$Vs = \sqrt{V_{ds}^2 + V_{qs}^2} = 1 \qquad V_{qs} = 1.0 \text{ p.u.} \qquad (13)$$

Applying these initial conditions to equation (4) under steady state open-circuit conditions gives.

$$V_{qs} = \omega_r \lambda_{ds} \quad \text{or} \quad I_{fr} = \frac{V_{qs}}{X_{md}} = \frac{1}{X_{md}} \qquad (14)$$

Similarly, equation (5) becomes

$$V_{fr} = r_{fr} I_{fr} = \frac{V_{qs} r_{fr}}{X_{md}} = \frac{r_{fr}}{X_{md}} \qquad (15)$$

The above equations were recalled to simulate for constant speed that could be compared with variable speed condition where different damping components were applied.

II DERIVING MODELS FOR VARIABLE SPEED SIMULATION

It is easy to see that the total inertia of the driving motors is only $2J_{DC}$ since both are rigidly coupled together. If the speed of the DC motor combination is ω_{DC} and that of the driven synchronous generator is ω_{gen}, then the ratio of the two speeds is proportional to the gear ratio:

$$K = \frac{\omega_{GEN}}{\omega_{DC}} \qquad (16)$$

If frictional losses in the transmission are neglected, and it is assumed that the inertia of the gear system is negligible, the kinetic energy due to the equivalent inertia seen by the DC motors J_{EFF}_DC must be equal to the total kinetic energy of the various moving parts. This implies

International Journal of Engineering Research & Technology (IJERT)
ISSN: 2278-0181
Vol. 5 Issue 01, January-2016

$$\frac{1}{2} J_{EFF\ -DC}\ \omega_{DC}^2 = \frac{1}{2}(2J_{DC})\omega_{DC}^2 + \frac{1}{2} J_{GEN}\,\omega_{GEN}^2 \quad (17)$$

Combining equation (14) and (15), the effective inertia of the entire drive system referred to the DC motor side is

$$J_{EFF\_DC} = 2J_{DC} + K^2 J_{GEN} \quad (18)$$

In a similar manner, the effective inertia referred to the generator side would be

$$J_{EFF\_GEN} = 2K^2 J_{DC} + J_{GEN} \quad (19)$$

The inertia of the two rotating masses (DC motor set and synchronous machine) and the torsional spring constant of the connecting shaft (and the flexible coupling) have a natural frequency of vibration ω_o at which the two masses tend to oscillate in opposition to each other. The stresses in the shaft are twisting stresses that load the shaft in shear. To evaluate the Oscillating shaft torque T_{SH} at the flexible coupling, the torque equation for both rotating masses with their oscillation angles γ_{DC} and γ_{GEN} are related by two second –order differential equations. **[6]**.

$$K^2 J_{GEN} \frac{d^2\gamma_{GEN}(\tau)}{d\tau^2} - T_{SH}(\tau) = 0 \quad (20)$$

$$2J_{DC} \frac{d^2\gamma_{DC}(\tau)}{d\tau^2} + T_{SH}(\tau) = T_{EX}(\tau) \quad (21)$$

Where the shaft torque is given by

$$T_{SH}(\tau) = C(\gamma_{DC}(\tau) - \gamma_{GEN}(\tau) \quad (22)$$

$T_{ex}(\tau)$ appearing in equation (21) is the exciting torque, which, for the purpose of this study, is the synchronous machine short-circuit torque given in equation (10), and C is the spring constant.

Equations (20) and (21) can be combined and written as

$$\frac{d^2\gamma_{DC}(\tau)}{d\tau^2} - \frac{d^2\gamma_{GEN}(\tau)}{d\tau^2} = -\left(\frac{1}{2J_{DC}} + \frac{1}{K^2 J_{GEN}}\right) T_{SH}(\tau) + \frac{T_{EX}(\tau)}{2J_{DC}} \quad (23)$$

If the effective shaft angle is represented as

$$\gamma(\tau) = \gamma_{DC}(\tau) - \gamma_{GEN}(\tau) \quad (24)$$

Then equation (3.44) can be written as

$$\frac{d^2\gamma(\tau)}{d\tau^2} + \omega_0^2\gamma(\tau) = \frac{T_{EX}(\tau)}{2J_{DC}} \quad (25)$$

Where the resonant frequency ω_o, now appearing in equation (25), is given by

$$\omega_o = \sqrt{\frac{C - (2J_{DC} + K^2 J_{GEN})}{(2J_{DC} - K^2 J_{GEN})}} \quad (26)$$

Finally, a damping term (in the coupling) can now be included and then the resulting dynamic equation of the effective shaft angle becomes

$$\frac{d^2\gamma(\tau)}{d\tau^2} + h\frac{d\gamma(\tau)}{d\tau} + w_0^2\gamma(\tau) = \frac{T_{EX}(\tau)}{2J_{DC}} \quad (27)$$

Where $h = \frac{2Dc}{\omega_o}$

$D = \frac{0.01}{(2\pi)}$ for steel coupling and

D = 0.1/(2π) for rubber coupling. **[7].** The solution of equation (27) will ultimately depend on the nature of the disturbance (exciting torque).

A Simulation of the System

It is known that the frequency of the exciting torque ω should be far from the resonant frequency ω_0 in order to avoid torsional resonance of the drive system, which is capable of creating very high shaft torque that could break the couplings. For this reason, the study will consider the value of $\omega_0 = \frac{1}{2}\omega$. However, the response of shaft torque due to variations in ω_0 and the spring constant ‘‘ c’’ will be studied. An SSC performance can be observed by setting $V_{qs} = V_{ds} = 0$ after the output voltage has settled to 1.0 p.u. The short circuit is performed at a point when the voltage waveform is at the maximum, the so-called best case. **[8]**. This ensures that the shortcircuit currents do not contain DC components, a situation that eases the procedure of transient parameter extraction from the short-circuit current waveforms. The simulations are performed using the commercial software **MATLAB Simulink® maths work Inc 2006**. Two broad conditions, viz, constant speed and variable speed, are considered. The variable-speed condition clearly emphasizes the inaccuracies arising from not keeping the speed constant during the period in which the SSC current and torque waveforms are captured.

B Variable Speed Simulation

The practicable case in which the generator is driven by the DC motors is now considered. Prior to commencement of the numerical solution in this case, the mechanical equation of the DC machine

$$\frac{d\omega}{d\tau} = -\frac{p}{J} T_{em}$$

International Journal of Engineering Research & Technology (IJERT)
ISSN: 2278-0181
Vol. 5 Issue 01, January-2016

Where,

P = Generator pole pairs

T_{em}= The driving turbine torque

J = Equivalent moment of inertia

γ = Rotor lag angle

has to be modified to :

$$\frac{d\omega_{m(\tau)}}{d\tau} = \frac{1}{J_{EFF}}\left(\varphi i_a - T_{SH}(\tau)\right) \ldots\ldots(28)$$

Where T_{BGEN} and T_{BDC} are, respectively, the rated base torques of the generator and the combined DC motor. There is no electrical connection between the DC motor and the generator, so Eq. (1) does not need any modification.

All of the synchronous generator, DC motor, and drive system equations are solved together. The solution of Eq. (27) with the generator torque T_{EX} (τ) gives the shaft angle γ (τ) with which the shaft torque T_{SH} (τ) can be computed using Eq. (22). The resulting shaft torque is then used in the solution of Eqs. (1) and (28) to obtain the speed of the DC motor that now drives the generator. The following four conditions are investigated for the variable-speed simulations.

III WHEN THE SYSTEM IS RIGIDLY COUPLED

A *The generator is rigidly coupled to the DC machine through the gear only.*

In this case, there is no spring coupling. The shaft torque then equals the short circuit torque (T_{SH} in Eq. (28) is replaced by T_{EX} for this case). The mechanical equation of shaft coupling dynamics in Eq. (27) is not included in the model equations to be solved in this case. The various oscilogram or the envelop under the rigid coupling condition is shown below

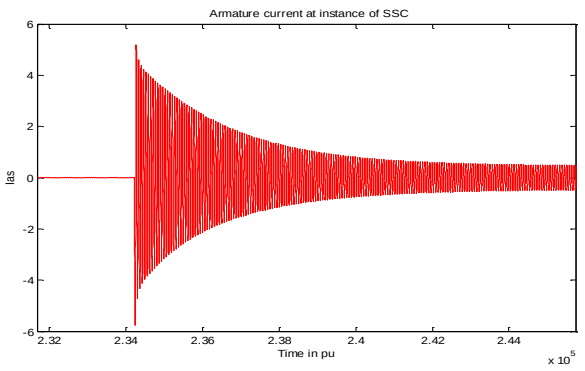

Figure 1 I_{as} at constant speed at SSC

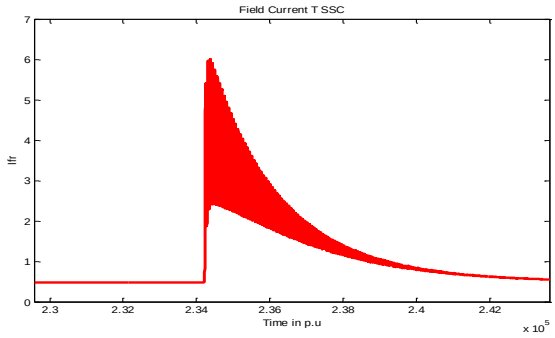

Figure 2 I_{fr} at constant speed when SSC occured

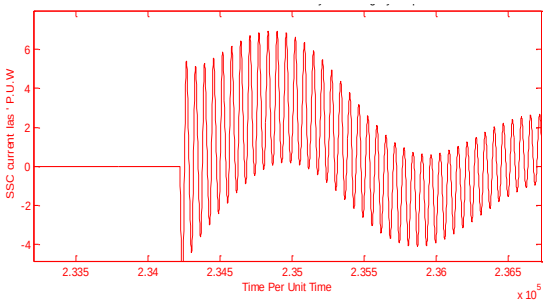

Figure 3 Effect of short circuit on I_{as} when the system is rigidly coupled

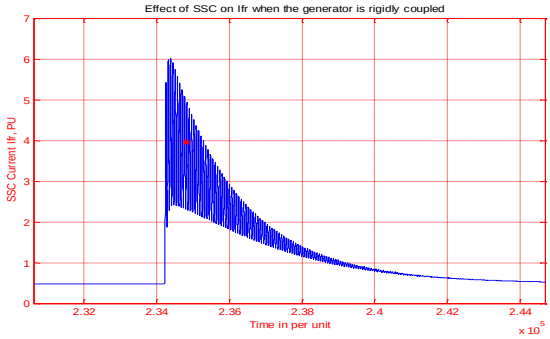

Figure 4 Effect of short circuit on I_{fr} when the generator is rigidly coupled

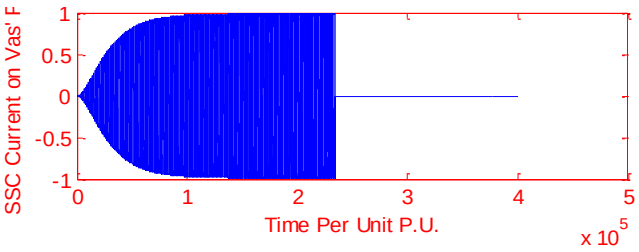

Figure 5 Effect of short circuit on generator's armature voltage when the system is rigidly coupled

IV THE GENERATOR IS COUPLED TO THE DC MACHINE WHEN THE DAMPING IS ZERO(0.0)

The generator is coupled to the DC machine through a gear, but no damping is included. All the equation sets are solved with D = 0. This modifies the nature of Eq. (27). The various envelops or oscilograms are shown below.

International Journal of Engineering Research & Technology (IJERT)
ISSN: 2278-0181
Vol. 5 Issue 01, January-2016

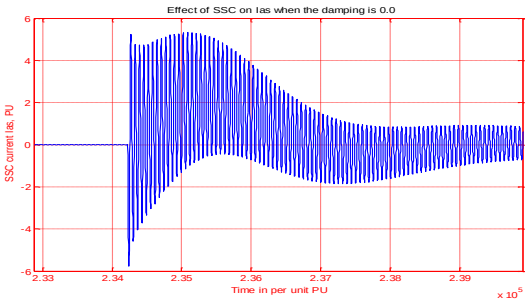

Figure 6 Effect of short circuit on I_{as} when the damping is 0.0

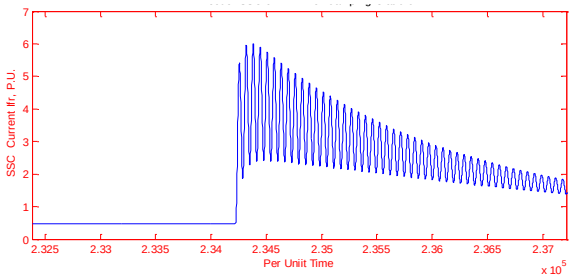

Figure 7 Effect of sudden short circuit on I_{fr} when the damping is 0.0

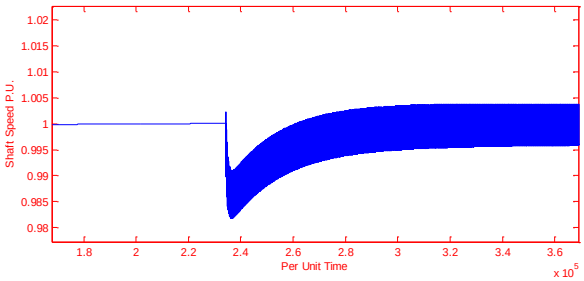

Figure 8 Speed departure from synchronism at short circuit when the damper is 0.0

V THE GENERATOR IS COUPLED TO THE DC MACHINE WHEN THE DAMPING IS 0.1

The steel coupling is set that $D = \frac{0.1}{(2\pi)}$, and all equations are solved. The corresponding oscillograms after simulation are shown below

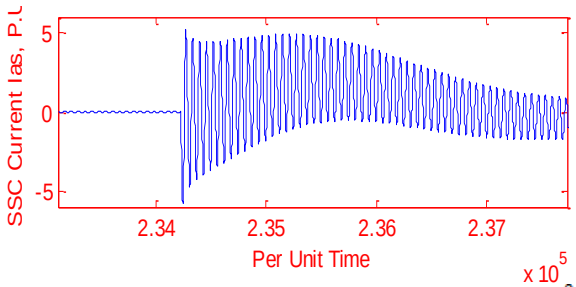

Figure 9 Effect of short circuit on I_{as} when the damping is $D = \frac{0.1}{(2\pi)}$

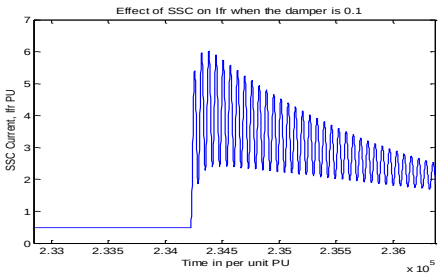

Figure 10 I_{fr} current at short circuit when the damper is $\frac{0.1}{(2\pi)}$

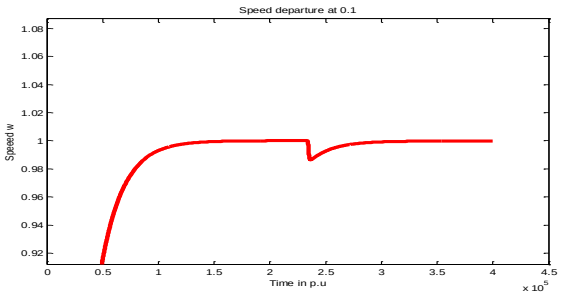

Figure 11 Speed characteristics when the damping is $\frac{0.1}{(2\pi)}$

VI THE GENERATOR IS COUPLED TO THE DC MACHINE WHEN THE DAMPING IS 0.01

The rubber coupling is at $D = \frac{0.01}{(2\pi)}$, and all equations are also solved.when the generator is coupled to the DC motors with the damping set at $D = \frac{0.01}{(2\pi)}$ the following characteristics were obtained sudden short circuit.Figure 12 Effect of short circuit on I_{as} when the damper is at $\frac{0.01}{(2\pi)}$

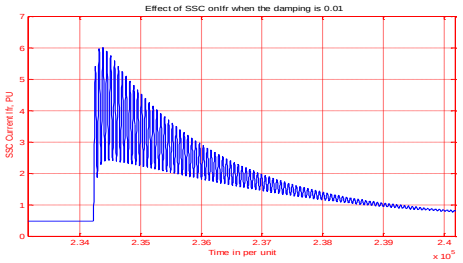

Figure 13 I_{fr} Characteristic at short circuit when the damper is $\frac{0.01}{(2\pi)}$

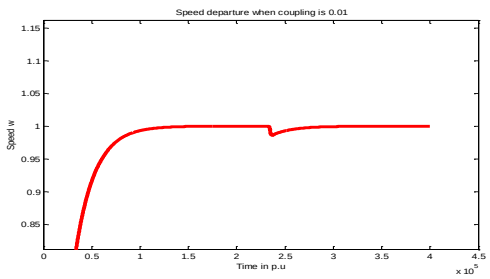

Figure 14 Speed w_m deviation at short circuit when the damper is $\frac{0.01}{(2\pi)}$

International Journal of Engineering Research & Technology (IJERT)
ISSN: 2278-0181
Vol. 5 Issue 01, January-2016

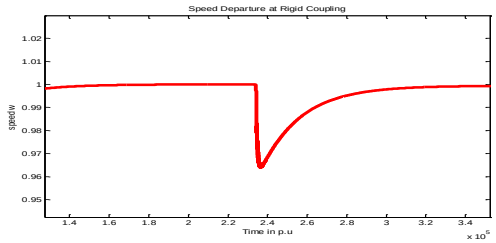

Figure 15 Speed departure at SSC when the machine is rigidly coupled.

VII ARMATURE CURRENT OF THE GENERATOR (I_{AS})

The stator current waveforms for the constant-speed operation of figure 1, shows that at the point of the short circuit, the current rose spontaneously and decayed rapidly. This point is the sub-transient region which degenerated to the transient period of the oscillogram. The various regions in which the transients occurred are recorded in the section that discussed the extraction of the parameters. The rubber coupling of Figure 9 and figure 12 look alike. However, some differences exist between these and can only be appreciated when the transient parameters have been extracted from each curve and compared. At the sub transient region, the current decayed fastly and at the transient region, the current tends to rise before coming to the steady state condition. The parameter extraction has shown the major difference between the two different envelop. Figures 3 and 6 indicate that these oscillated very well before settling to final values. Under this condition, it is difficult to ascertain the transient region from the oscillograph. However, their steady state and subtransient regions were captured.

A Field Currents (I_{fr})

Figures 2, 4, 7, 10 and 13 depicts the rotor field current when sudden short circuit occurred at the terminals of the generator driven by the two DC motors. The five oscillograms or envelop looks alike but the envelop captured during the de excitation of the machine comparatively analyze their differences. Between the subtransient and the transient region, the oscillogram shows a sharp rise in short circuit current before dropping to steady state condition.

Careful observation shows that the rigid coupling and when the damper is 0.01 decayed faster to steady state than the other envelops.

Table 1 shows the field current at different time intervals. The table also reveal the closeness of the field current at various condition of the machine.

Table 1 Field current during short circuit captured at various conditions

S/N	Condition of the Generator	I_{fr} at Normal (Amps)
1	Constant Speed	5.885
2	D = 0.0	5.960
3	D = 0.1	5.828
4	D = 0.01	5.899
5	Rigid Coupling	5.910

VIII EFFECT OF SUDDEN SHORT CIRCUIT ON THE SPEED OF THE SYSTEM

Figures 8, 11, 14 and 15 show the extent of speed departures from synchronous conditions following SSC on the terminals of the generator. The ideal case of constant speed is not represented in table 2 since there is no speed departure. The speed departure for the steel coupling appears to be the average of that of the undamped case a short while after the SSC, even though the corresponding current curves are remarkably similar. A general observation is that for even very low speed departure, significant shaft torques result; the farther the speed deviates from synchronous, the longer it takes the system to attain steady-state mode, and the more the current waveforms oscillate. In all the cases, the short circuit is arranged to occur when the machine voltage has built up to 1.0 p.u. in steady state and at a time when the voltage wave is a maximum. The table below shows the various point of departure from synchronism.

Table 2 Speed departure characteristics from synchronism at the point of short circuit.

S/N	STATE OF THE SYSTEM	SPEED W (pu)
1	Constant speed	-
2	D = 0.0	0.9929
3	D = $\frac{0.1}{2\pi}$	0.9963
4	D = $\frac{0.01}{2\pi}$	0.9866
6	Rigid Coupling	0.9779

IX EXTRACTED PARAMETERS AT CONSTANT AND VARIABLE SPEED CONDITIONS

The conditions at which the speed deviates from constancy or out of synchronism during short circuit of the generator in which different coupling methods were adopted were studied and parameters of the generator were extracted at the conditions of sub transients, transients and steady state as shown in the table below.

International Journal of Engineering Research & Technology (IJERT)
ISSN: 2278-0181
Vol. 5 Issue 01, January-2016

Table 3 Summary of Extracted Parameters

Extracted Values					
Parameters	Constant Speed	Rigid coupling	D = 0	$D = \frac{0.1}{2\pi}$	$D = \frac{0.01}{2\pi}$
$x_d\ (p.u)$	2.1978	2.181	2.1978	2.197	2.1973
$x'_d(p.u)$	0.217	-	-	0.2156	-
$x''_d(p.u)$	0.1923	0.1854	1.9105	0.1926	0.1917
$\tau'_d(sec)$	0.021 sec	-	-	0.109 sec	-
$\tau''_d(sec)$	0.001	0.018sec	0.018 sec	0.019 sec	0.018 sec
$\mathbf{I_{as}}$ (Final)	0.4548	0.4585	0.455	0.4551	0.4551
I'_{as} (Transient)	4.600	-	-	4.638	-
I''_{as} **(SusubTransient)**	5.200	5.393	5.234	5.192	5.216

A Analysis of the Waveforms.

The stator current waveforms for the constant-speed operation of figure 1, shows that at the point of the short circuit, the current rose spontaneously and decayed rapidly. This point is the sub-transient region which degenerated to the transient period of the oscillogram. The various regions in which the transients occurred are recorded in the section that discussed the extraction of the parameters. The rubber coupling of Figure 9 and figure 12 look alike. However, some differences exist between these and is appreciated at table 3 where transient parameters extraction from each curve have treated and compared. At the sub transient region, the current decayed fastly and at the transient region, the current tends to rise before coming to the steady state condition. The parameter extraction has shown the major difference between the two different envelop. Figures 3 and 6 indicate that these oscillated very well before settling to final values. Under this condition, it is difficult to ascertain the transient region from the oscillograph. However, their steady state and subtransient regions were captured. Comparing table 3, it is noticed that when the speed is constant, at subtransient level, the current rise spontaneously and decay spontaneously to transient condition and finally to steady state condition. Unlike the constant speed conditions, the variable speed, where different coupling methods were adopted, this impacted deeply on the speed of the rotor. This is attested from the oscillogram of the captured envelops at the time of sudden short circuit on the machine. This resulted in the longer time it took the machine to settle to steady state position otherwise known as the recovery condition of the machine.

X CONLUSION

In spite of synchronous generators long history of operation, the research work presented hitherto have not put forward fully sufficient comparative studies with regard to sudden short circuits of the machine. This can be due to the fact that short circuit faults occurring during operation cannot offer sufficient information with a view to fault correct assessment, simply because of the various circumstances in which these faults do practically occur. Using a number of basic building blocks easily found in the Mathlab Simulink® library, it is possible to simulate the fault analysis and study its dynamic response using the graphical displays through the oscillogram from the scope block. The graphical results from the time the fault occurred was then observed and the parameters were extracted from the graph analysis. The simulink models parameters extraction of the synchronous machine are then verified as the results from the oscillograms studied can be used to extract accurate parameters for the synchronous machine. The case in which a rubber coupling is used $\left(D = \frac{0.1}{2\pi}\right)$ gives the best results here. Under that condition, the shear stresses on the shaft are minimal as the rubber provides sufficient flexibility. The speed is nearly constant, even after short circuit.

XI REFERENCES

[1] E. Kyriakides, G. T. Heydt, and V. Vittal, "On-line estimation of synchronous generator parameters using a damper current observer and a graphic user interface," *IEEE Trans. Energy Convers.*, vol. 19, no. 3, pp. 499–507, Sep. 2004.

[2] E. Kyriakides, G. T. Heydt, and V. Vittal, "On-line parameter estimation of round rotor synchronous generators including magnetic saturation,"*IEEE Trans.Energy Convers.*,vol. 20, no.3,pp.529–537, Sep. 2005

[3] L. A. Kilgore, "Calculation of synchronous machine constants," AIEE Trans., vol. 50, pp.1201– 1214,Dec. 1931.

[4] S. H. Wright, "Determination of synchronous machine constants by test," AIEE Trans., vol. 50, pp. 1331–1351, Dec. 1931

[5] Test Procedures for Synchronous Machines, Part I— cceptance and Performance Testing, Part II—Test Procedures and Parameter Determination for Dynamic Analysis.

[6] E. F. Merrill, "Dynamics of ac electrical machines," IEEE Trans. Industry Appl., Vol. 30, 350 No. 2, pp. 277–285, 1994.

[7] G. K. Dubey, ''Fundamentals of Electrical Drives'', New Delhi: Narosa Publishing House, PP506, 2001.

[8] B. Adkins, ''The General Theory of Electrical Machines'', London: Chapman and Hall, P36, 1964

[9] E.S Obe, ''Dynamics of a Turbo –genrator Driven by DC Motors during Off – line Three-phase Sudden Short Circuit. Electric Power Components and Systems, 39:1828-1844, Taylor & Francis Group, Informa Ltd LLC Office, Mortimer House, 37-41 Mortimer street, London WIT 3JH, UK, 2011.